



Stable and Efficient Galerkin Reduced Order Models for Non-Linear Fluid Flow

SAND2011-4383C

Irina Kalashnikova^{1,2} and Matthew F. Barone¹

¹ Sandia National Laboratories*, Albuquerque, NM, U.S.A.

² Institute for Computational & Mathematical Engineering (iCME),
Stanford University, Stanford, CA, U.S.A.

6th AIAA Theoretical Fluid Mechanics Conference
Honolulu, HI
Monday, June 27, 2011

* Sandia is a multiprogram laboratory operated by Sandia Corporation, a Lockheed Martin Company, for the United States Department of Energy under Contract DE-AC04-94AL85000.





Why Develop a Fluid Reduced Order Model (ROM)?

CFD modeling of unsteady
3D flows is expensive!



Why Develop a Fluid Reduced Order Model (ROM)?

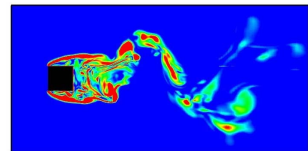
CFD modeling of unsteady 3D flows is expensive!

A **Reduced Order Model (ROM)** is a surrogate numerical model that aims to capture the essential dynamics of a full model but with far fewer dofs.

Why Develop a Fluid Reduced Order Model (ROM)?

CFD modeling of unsteady 3D flows is expensive!

A Reduced Order Model (ROM) is a surrogate numerical model that aims to capture the essential dynamics of a full model but with far fewer dofs.



Applications in Fluid Dynamics:

- Predictive modeling across a parameter space (e.g., aeroelastic flutter analysis).
- System modeling for active flow control.
- Long-time unsteady flow analysis, e.g., fatigue of a wind turbine blade under variable wind conditions.





Motivation for Numerical Analysis of ROMs

Use of ROMs in predictive applications raises questions about their stability & convergence.

- Projection ROM approach is an alternative discretization of the governing PDEs.
- Desired numerical properties of a ROM discretization:
 - ▶ **Consistency** (with continuous PDEs):
 - ▶ **Stability**:
 - ▶ **Convergence**: requires consistency and stability.



Motivation for Numerical Analysis of ROMs

Use of ROMs in predictive applications raises questions about their stability & convergence.

- Projection ROM approach is an alternative discretization of the governing PDEs.
- Desired numerical properties of a ROM discretization:
 - ▶ **Consistency** (with continuous PDEs): loosely speaking, a ROM **CAN** be consistent with respect to the full simulations used to generate it.
 - ▶ **Stability**:
 - ▶ **Convergence**: requires consistency and stability.



Motivation for Numerical Analysis of ROMs

Use of ROMs in predictive applications raises questions about their stability & convergence.

- Projection ROM approach is an alternative discretization of the governing PDEs.
- Desired numerical properties of a ROM discretization:
 - ▶ **Consistency** (with continuous PDEs): loosely speaking, a ROM **CAN** be consistent with respect to the full simulations used to generate it.
 - ▶ **Stability**: numerical stability is **NOT** in general guaranteed *a priori* for a ROM!
 - ▶ **Convergence**: requires consistency and stability.



Motivation for Numerical Analysis of ROMs

Use of ROMs in predictive applications raises questions about their stability & convergence.

- Projection ROM approach is an alternative discretization of the governing PDEs.
- Desired numerical properties of a ROM discretization:
 - ▶ **Consistency** (with continuous PDEs): loosely speaking, a ROM **CAN** be consistent with respect to the full simulations used to generate it.
 - ▶ **Stability**: numerical stability is **NOT** in general guaranteed *a priori* for a ROM!
 - ▶ **Convergence**: requires consistency and stability.

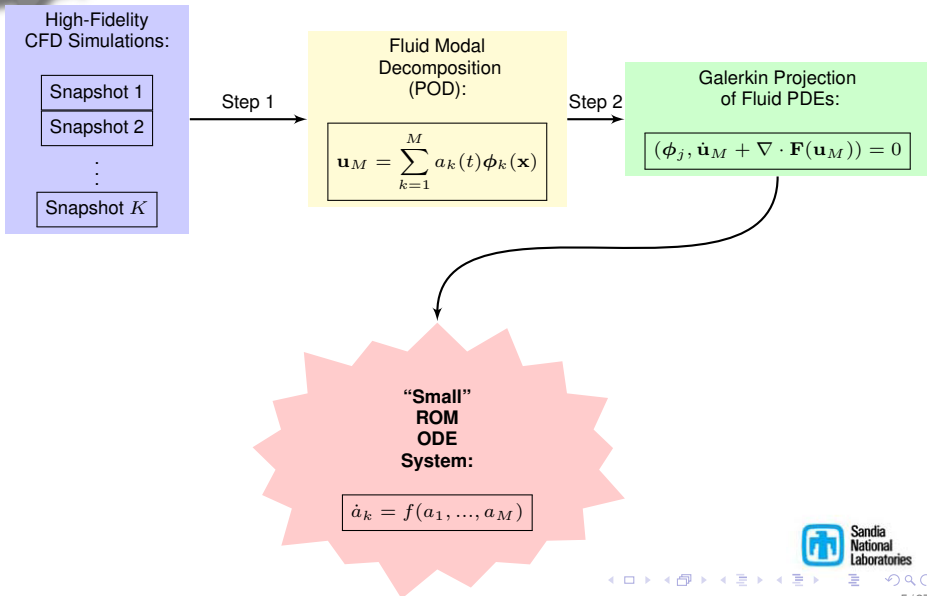
This talk focuses on how to construct a Galerkin ROM that is **stable *a priori***



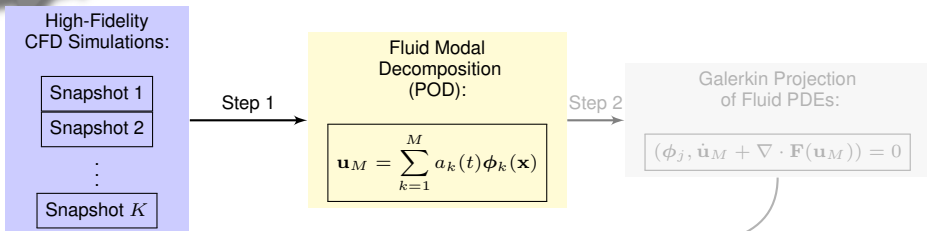
Outline

- 1 POD/Galerkin Approach to Model Reduction
- 2 Numerical Stability
- 3 A Stable ROM for the Linearized Compressible Euler Equations
 - Symmetrized Equations and Energy Stability
 - Numerical Studies
- 4 A Stable ROM for the Full Compressible Navier-Stokes Equations
 - Symmetrized Equations and Entropy Stability
 - Interpolation of Non-Linear Terms
 - Preliminary Numerical Studies
- 5 Summary & Future Work
- 6 References
- 7 Appendix

Model Reduction Approach



Step 1: Constructing the Modes



- **POD basis** $\{\phi_i\}_{i=1}^M$ with $M \ll K$ maximizes the energy in the projection of snapshots onto $\text{span}\{\phi_i\}$.
- **POD eigenvalue problem:**

$$\mathbf{R}\phi = \lambda\phi$$

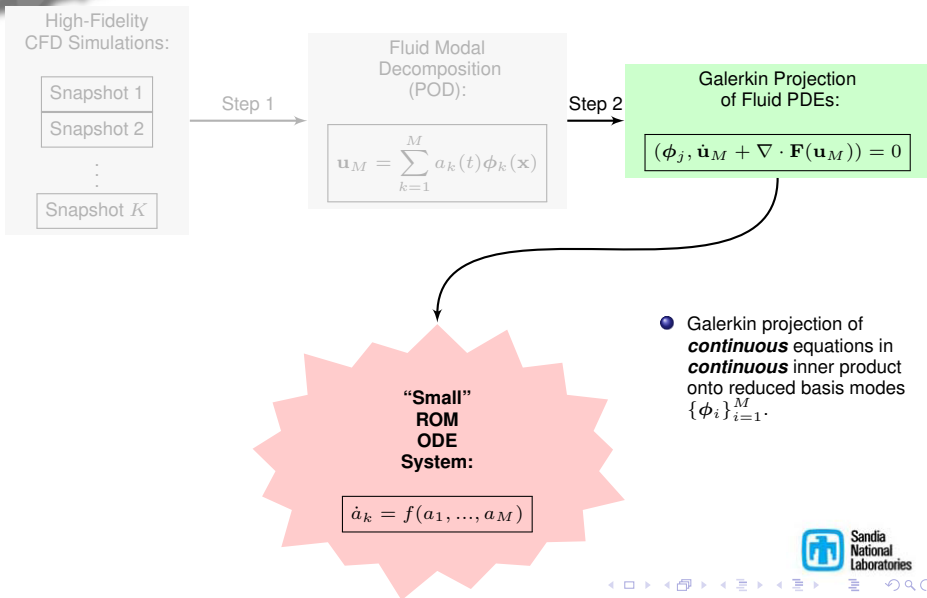
where $\mathbf{R}\phi \equiv \langle \mathbf{u}^k(\mathbf{u}^k, \phi) \rangle$.

“Small”
ROM
ODE
System:

$$\dot{a}_k = f(a_1, \dots, a_M)$$



Step 2: Galerkin Projection





Stability Definitions

- **Practical Definition:** Numerical solution does not “blow up” in finite time.



Stability Definitions

- **Practical Definition:** Numerical solution does not “blow up” in finite time.
- **More Precise Definition:** Numerical discretization does not introduce any spurious instabilities inconsistent with natural instability modes supported by the governing continuous PDEs.



Stability Definitions

- **Practical Definition:** Numerical solution does not “blow up” in finite time.
- **More Precise Definition:** Numerical discretization does not introduce any spurious instabilities inconsistent with natural instability modes supported by the governing continuous PDEs.

Numerical solutions **must** obey conservation laws
satisfied by solutions of continuous equations

Stability Definitions

- **Practical Definition:** Numerical solution does not “blow up” in finite time.
- **More Precise Definition:** Numerical discretization does not introduce any spurious instabilities inconsistent with natural instability modes supported by the governing continuous PDEs.

Numerical solutions **must** obey conservation laws satisfied by solutions of continuous equations

Linearized Compressible Euler Equations:

$$\frac{dE}{dt} \leq 0$$

Non-increasing energy

Compressible Navier-Stokes Equations:

$$\frac{d}{dt} \int_{\Omega} \rho \eta d\Omega \geq 0$$

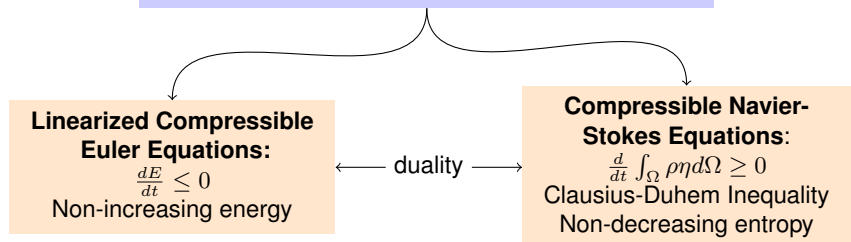
Clausius-Duhem Inequality
Non-decreasing entropy

← duality →

Stability Definitions

- **Practical Definition:** Numerical solution does not “blow up” in finite time.
- **More Precise Definition:** Numerical discretization does not introduce any spurious instabilities inconsistent with natural instability modes supported by the governing continuous PDEs.

Numerical solutions **must** obey conservation laws satisfied by solutions of continuous equations



- Analyzed using the **Energy Method**: Uses an equation for the evolution of numerical solution “energy” (or “entropy”) to determine stability.

3D Linearized Compressible Euler Equations

- Useful for aero-elasticity, aero-acoustics, flow instability analysis.
- Linearization of full compressible Euler equations:

$$\mathbf{q}^T(\mathbf{x}, t) \equiv \begin{pmatrix} u_1 & u_2 & u_3 & \zeta & p \end{pmatrix} \equiv \underbrace{\bar{\mathbf{q}}^T(\mathbf{x})}_{\text{mean}} + \underbrace{\mathbf{q}'^T(\mathbf{x}, t)}_{\text{fluctuation}} \in \mathbb{R}^5$$

$$\Rightarrow \mathbf{q}'_{,t} + \mathbf{A}_i \mathbf{q}'_{,i} + \mathbf{C} \mathbf{q}' = \mathbf{0}$$

where

$$\mathbf{A}_1 = \begin{pmatrix} \bar{u}_1 & 0 & 0 & 0 & \bar{\zeta} \\ 0 & \bar{u}_1 & 0 & 0 & 0 \\ 0 & 0 & \bar{u}_1 & 0 & 0 \\ -\bar{\zeta} & 0 & 0 & \bar{u}_1 & 0 \\ \gamma \bar{p} & 0 & 0 & 0 & \bar{u}_1 \end{pmatrix}, \quad \mathbf{A}_2 = \begin{pmatrix} \bar{u}_2 & 0 & 0 & 0 & 0 \\ 0 & \bar{u}_2 & 0 & 0 & \bar{\zeta} \\ 0 & 0 & \bar{u}_2 & 0 & 0 \\ 0 & -\bar{\zeta} & 0 & \bar{u}_2 & 0 \\ 0 & \gamma \bar{p} & 0 & 0 & \bar{u}_2 \end{pmatrix}$$

$$\mathbf{A}_3 = \begin{pmatrix} \bar{u}_3 & 0 & 0 & 0 & 0 \\ 0 & \bar{u}_3 & 0 & 0 & 0 \\ 0 & 0 & \bar{u}_3 & 0 & \bar{\zeta} \\ 0 & 0 & -\bar{\zeta} & \bar{u}_3 & 0 \\ 0 & 0 & \gamma \bar{p} & 0 & \bar{u}_3 \end{pmatrix}, \quad \mathbf{C} = \begin{pmatrix} \bar{u}_{1,1} & \partial \bar{u}_{1,2} & \bar{u}_{1,3} & \bar{p}_{,1} & 0 \\ \bar{u}_{2,1} & \bar{u}_{2,2} & \bar{u}_{2,3} & \bar{p}_{,2} & 0 \\ \bar{u}_{3,1} & \bar{u}_{3,2} & \bar{u}_{3,3} & \bar{p}_{,3} & 0 \\ \bar{\zeta}_{,1} & \bar{\zeta}_{,2} & \bar{\zeta}_{,3} & -\nabla \cdot \bar{\mathbf{u}} & 0 \\ \bar{p}_{,1} & \bar{p}_{,2} & \bar{p}_{,3} & 0 & 0 \end{pmatrix}$$

Symmetrized Compressible Euler Equations & Symmetry Inner Product

Energy stability of the Galerkin ROM can be proven* following a “symmetrization” of the linearized compressible Euler equations.

- Linearized hyperbolic compressible Euler system is “symmetrizable”.
- Pre-multiply equations by symmetric positive definite matrix:

$$\mathbf{H} = \begin{pmatrix} \bar{\rho} & 0 & 0 & 0 & 0 \\ 0 & \bar{\rho} & 0 & 0 & 0 \\ 0 & 0 & \bar{\rho} & 0 & 0 \\ 0 & 0 & 0 & \alpha^2 \gamma \bar{\rho}^2 \bar{p} & \bar{\rho} \alpha^2 \\ 0 & 0 & 0 & \bar{\rho} \alpha^2 & \frac{1+\alpha^2}{\gamma \bar{p}} \end{pmatrix} \Rightarrow \boxed{\mathbf{H}\mathbf{q}'_{,t} + \boxed{\mathbf{H}\mathbf{A}_i \mathbf{q}'_{,i}} + \mathbf{H}\mathbf{C}\mathbf{q}' = \mathbf{0}}$$

- \mathbf{H} is called the “symmetrizer” of the system: $\mathbf{H}\mathbf{A}_i$ are all symmetric.
- Define the “symmetry” inner product and “symmetry” norm:

$$(\mathbf{q}'^{(1)}, \mathbf{q}'^{(2)})_{(\mathbf{H}, \Omega)} \equiv \int_{\Omega} [\mathbf{q}'^{(1)}]^T \mathbf{H} \mathbf{q}'^{(2)} d\Omega, \quad \|\mathbf{q}'\|_{(\mathbf{H}, \Omega)} \equiv (\mathbf{q}', \mathbf{q}')_{(\mathbf{H}, \Omega)}$$

* M.F. Barone, D.J. Segalman, H. Thornquist, I. Kalashnikova. “Galerkin Reduced Order Models for Compressible Flow with Structural Interaction”. AIAA Paper No. 2008-0612, 46th AIAA Aerospace Science Meeting and Exhibit, Reno, NV (Jan. 2008); [2-4].



A Stable Galerkin ROM

- Stability analysis dictates that we use the symmetry inner product to compute the POD modes and perform the Galerkin projection.



A Stable Galerkin ROM

- Stability analysis dictates that we use the symmetry inner product to compute the POD modes and perform the Galerkin projection.
- Energy estimate: $\|\mathbf{q}'_M(\mathbf{x}, t)\|_{(\mathbf{H}, \Omega)} \leq e^{\beta t} \|\mathbf{q}'_M(\mathbf{x}, 0)\|_{(\mathbf{H}, \Omega)}$.



A Stable Galerkin ROM

- Stability analysis dictates that we use the symmetry inner product to compute the POD modes and perform the Galerkin projection.
- Energy estimate: $\|\mathbf{q}'_M(\mathbf{x}, t)\|_{(\mathbf{H}, \Omega)} \leq e^{\beta t} \|\mathbf{q}'_M(\mathbf{x}, 0)\|_{(\mathbf{H}, \Omega)}$.

Practical Implication:

Symmetry inner product ensures Galerkin projection step of the ROM is stable for **any** basis!



A Stable Galerkin ROM

- Stability analysis dictates that we use the symmetry inner product to compute the POD modes and perform the Galerkin projection.
- Energy estimate: $\|\mathbf{q}'_M(\mathbf{x}, t)\|_{(\mathbf{H}, \Omega)} \leq e^{\beta t} \|\mathbf{q}'_M(\mathbf{x}, 0)\|_{(\mathbf{H}, \Omega)}$.

Practical Implication:

Symmetry inner product ensures Galerkin projection step of the ROM is stable for **any** basis!

- **Stability-Preserving Discrete Implementation:**

- ▶ Define snapshots and POD modes using piecewise smooth finite elements.
- ▶ Apply Gauss quadrature rules of sufficient accuracy to compute exactly inner products.
- ▶ Fairly general, works for any nodal mesh that can be represented using finite elements.

A Stable Galerkin ROM

- Stability analysis dictates that we use the symmetry inner product to compute the POD modes and perform the Galerkin projection.
- Energy estimate: $\|\mathbf{q}'_M(\mathbf{x}, t)\|_{(\mathbf{H}, \Omega)} \leq e^{\beta t} \|\mathbf{q}'_M(\mathbf{x}, 0)\|_{(\mathbf{H}, \Omega)}$.

Practical Implication:

Symmetry inner product ensures Galerkin projection step of the ROM is stable for **any** basis!

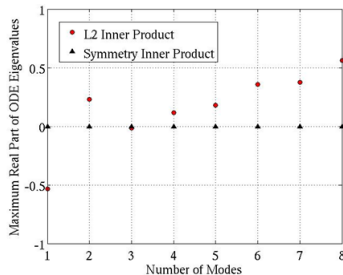
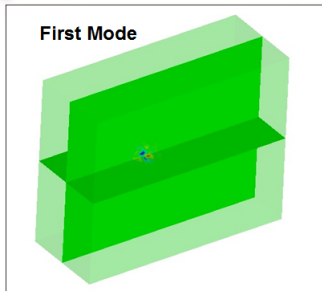
• Stability-Preserving Discrete Implementation:

- ▶ Define snapshots and POD modes using piecewise smooth finite elements.
- ▶ Apply Gauss quadrature rules of sufficient accuracy to compute exactly inner products.
- ▶ Fairly general, works for any nodal mesh that can be represented using finite elements.

A computer code was written that reads in the snapshot data written by AERO-F*, assembles the necessary finite element representation of the snapshots, computes the numerical quadrature for evaluation of the inner products, and projects the equations onto the modes.

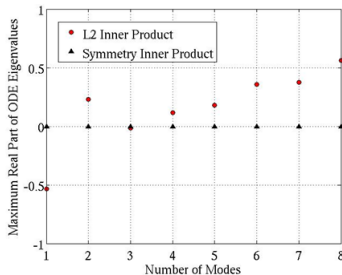
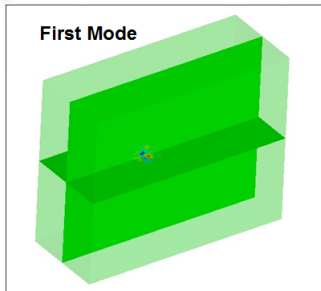
* AERO-F is an arbitrary Lagrangian–Eulerian code that can be used for high-fidelity aeroelastic analysis (Lieu, Farhat *et al.*).

Numerical Study 1: Purely Random Basis



- Uniform base flow: physically stable to any linear disturbance.
- Each mode is a random disturbance field that decays to 0 at the domain boundaries.
- Model problem for modes dominated by numerical error: extreme case of “bad” modes.

Numerical Study 1: Purely Random Basis



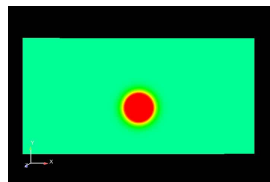
- Uniform base flow: physically stable to any linear disturbance.
- Each mode is a random disturbance field that decays to 0 at the domain boundaries.
- Model problem for modes dominated by numerical error: extreme case of “bad” modes.
- To test *a posteriori* the **stability** of a ROM dynamical system $\dot{\mathbf{a}}_M = \mathbf{K}\mathbf{a}_M$, check the Lyapunov condition:

$$\max_i \mathcal{R}\{\lambda_i(\mathbf{K})\} \leq 0?$$



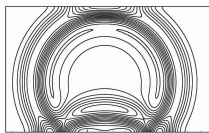
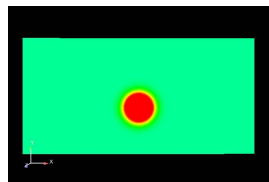
Numerical Study 2: 2D Pressure Pulse

- Reflection of cylindrical Gaussian pressure pulse in uniform base flow, $M_\infty = 0.25$.



Numerical Study 2: 2D Pressure Pulse

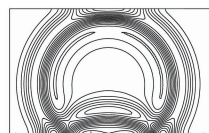
- Reflection of cylindrical Gaussian pressure pulse in uniform base flow, $M_\infty = 0.25$.
- Good qualitative agreement between CFD solution and 6 mode symmetry ROM (with BCs) on large scale.
- Excellent agreement between CFD solution and 14 mode symmetry ROM (with BCs).
- Symmetry ROM (with BCs) is stable – vs. L^2 ROM, which experienced instability when more than 6 or 7 modes were used.



CFD



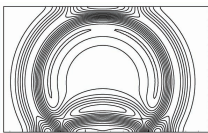
6 mode ROM



14 mode ROM

Numerical Study 2: 2D Pressure Pulse

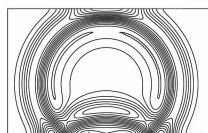
- Reflection of cylindrical Gaussian pressure pulse in uniform base flow, $M_\infty = 0.25$.
- Good qualitative agreement between CFD solution and 6 mode symmetry ROM (with BCs) on large scale.
- Excellent agreement between CFD solution and 14 mode symmetry ROM (with BCs).
- Symmetry ROM (with BCs) is stable – vs. L^2 ROM, which experienced instability when more than 6 or 7 modes were used.
- Symmetry ROM with BCs is convergent (*a priori* [2] and *a posteriori*).



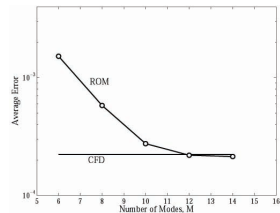
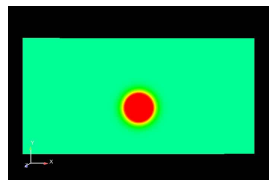
CFD



6 mode ROM



14 mode ROM



Full 3D Compressible Navier-Stokes Equations

- Required to describe satisfactorily compressible flows at transonic, supersonic and hypersonic Mach numbers where non-linear effects are significant.
- High accuracy simulations (DNS, LES) are required to capture correctly viscous and nonlinear effects (e.g., boundary layers, shocks, turbulence).
- Full compressible Navier-Stokes equations in the conservation variables:

$$\mathbf{U}^T(\mathbf{x}, t) \equiv (\rho \quad \rho u_1 \quad \rho u_2 \quad \rho u_3 \quad \rho e) \in \mathbb{R}^5$$

$$\Rightarrow \mathbf{U}_{,t} + \mathbf{A}_i \mathbf{U}_{,i} - (\mathbf{K}_{ij} \mathbf{U}_{,j})_{,i} = \mathbf{0}$$

where

$$\mathbf{F}_{i,i} = \mathbf{F}_{i,\mathbf{U}} \mathbf{U}_{,i} \equiv \mathbf{A}_i \mathbf{U}_{,i}, \quad \mathbf{F}_i^\nu \equiv \mathbf{K}_{ij}^\nu \mathbf{U}_{,j}, \quad \mathbf{F}_i^h \equiv \mathbf{K}_{ij}^h \mathbf{U}_{,j}$$

$$\mathbf{K}_{ij} \equiv \mathbf{K}_{ij}^\nu + \mathbf{K}_{ij}^h.$$

with

$$\mathbf{F}_i = u_i \mathbf{U} + p \underbrace{\begin{pmatrix} 0 \\ \delta_{1i} \\ \delta_{2i} \\ \delta_{3i} \\ u_i \end{pmatrix}}_{\text{Euler flux}}, \quad \mathbf{F}_i^\nu = \underbrace{\begin{pmatrix} 0 \\ \tau_{1i} \\ \tau_{2i} \\ \tau_{3i} \\ \tau_{ij} u_j \end{pmatrix}}_{\text{viscous flux}}, \quad \mathbf{F}_i^h = \underbrace{\begin{pmatrix} 0 \\ 0 \\ 0 \\ 0 \\ -q_i \end{pmatrix}}_{\text{heat flux}},$$



Entropy Variables & Entropy Stability

Entropy stability of the Galerkin ROM can be proven following a “symmetrization” of the compressible Navier-Stokes equations.

- Parabolic-hyperbolic compressible Navier-Stokes system is “symmetrizable”.

Theorem (Mock) [6]

A parabolic-hyperbolic system of conservation laws possesses a (convex) **generalized entropy function** $H(\mathbf{U})$ and becomes symmetric under the change of variables

$$\mathbf{V}^T = H_{,\mathbf{U}}$$



Entropy Variables & Entropy Stability

Entropy stability of the Galerkin ROM can be proven following a “symmetrization” of the compressible Navier-Stokes equations.

- Parabolic-hyperbolic compressible Navier-Stokes system is “symmetrizable”.

Theorem (Mock) [6]

A parabolic-hyperbolic system of conservation laws possesses a (convex) **generalized entropy function** $H(\mathbf{U})$ and becomes symmetric under the change of variables

$$\mathbf{V}^T = H_{,\mathbf{U}}$$

The variables \mathbf{V} are known as the **entropy variables**.

Entropy Variables & Entropy Stability

Entropy stability of the Galerkin ROM can be proven following a “symmetrization” of the compressible Navier-Stokes equations.

- Parabolic-hyperbolic compressible Navier-Stokes system is “symmetrizable”.

Theorem (Mock) [6]

A parabolic-hyperbolic system of conservation laws possesses a (convex) **generalized entropy function** $H(\mathbf{U})$ and becomes symmetric under the change of variables

$$\mathbf{V}^T = H_{,\mathbf{U}}$$

The variables \mathbf{V} are known as the **entropy variables**.

- Examples of entropy functions:

- Scalar conservation law (e.g., Burgers' equation): $H(\mathbf{U}) = \frac{u^2}{2}$.
- Shallow water equations: $H(\mathbf{U}) = \frac{1}{2}(gh^2 + |\mathbf{u}|^2h)$ [8].
- Compressible Euler equations: $H(\mathbf{U}) = Kp\rho^{-\gamma}$ [6].
- Compressible Navier-Stokes equations: $H(\mathbf{U}) = -\rho s$ [6, 9].

Entropy Variables & Entropy Stability

Entropy stability of the Galerkin ROM can be proven following a “symmetrization” of the compressible Navier-Stokes equations.

- Parabolic-hyperbolic compressible Navier-Stokes system is “symmetrizable”.

Theorem (Mock) [6]

A parabolic-hyperbolic system of conservation laws possesses a (convex) **generalized entropy function** $H(\mathbf{U})$ and becomes symmetric under the change of variables

$$\mathbf{V}^T = H_{,\mathbf{U}}$$

The variables \mathbf{V} are known as the **entropy variables**.

- Examples of entropy functions:

- Scalar conservation law (e.g., Burgers' equation): $H(\mathbf{U}) = \frac{u^2}{2}$.
- Shallow water equations: $H(\mathbf{U}) = \frac{1}{2}(gh^2 + |\mathbf{u}|^2h)$ [8].
- Compressible Euler equations: $H(\mathbf{U}) = Kp\rho^{-\gamma}$ [6].
- Compressible Navier-Stokes equations:** $H(\mathbf{U}) = -\rho s$ [6, 9].



Symmetrized Compressible Navier-Stokes Equations

- Compressible Navier-Stokes equations in the entropy variables:

$$\mathbf{V}^T(\mathbf{x}, t) \equiv \left(-U_5 + \rho_1(\gamma + 1 - s), \quad U_2, \quad U_3, \quad U_4, \quad -U_1 \right) \in \mathbb{R}^5$$

$$s = \ln \left[\frac{(\gamma - 1)\rho_1}{U_1^\gamma} \right], \quad \rho_1 = U_5 - \frac{1}{2U_1}(U_2^2 + U_3^2 + U_4^2)$$

$$\Rightarrow \mathbf{A}_0 \mathbf{V}_{,t} + \tilde{\mathbf{A}}_i \mathbf{V}_{,i} - (\tilde{\mathbf{K}}_{ij} \mathbf{V}_{,j})_{,i} = \mathbf{0}$$

where

$$\mathbf{A}_0 \equiv \mathbf{U}_{,\mathbf{V}}, \quad \tilde{\mathbf{A}}_i \equiv \mathbf{A}_i \mathbf{A}_0, \quad \tilde{\mathbf{K}}_{ij} \equiv \mathbf{K}_{ij} \mathbf{A}_0,$$



Symmetrized Compressible Navier-Stokes Equations

- Compressible Navier-Stokes equations in the entropy variables:

$$\mathbf{V}^T(\mathbf{x}, t) \equiv \left(-U_5 + \rho_1(\gamma + 1 - s), \quad U_2, \quad U_3, \quad U_4, \quad -U_1 \right) \in \mathbb{R}^5$$

$$s = \ln \left[\frac{(\gamma - 1)\rho_1}{U_1^\gamma} \right], \quad \rho_1 = U_5 - \frac{1}{2U_1}(U_2^2 + U_3^2 + U_4^2)$$

$$\Rightarrow \mathbf{A}_0 \mathbf{V}_{,t} + \tilde{\mathbf{A}}_i \mathbf{V}_{,i} - (\tilde{\mathbf{K}}_{ij} \mathbf{V}_{,j})_{,i} = \mathbf{0}$$

where

$$\mathbf{A}_0 \equiv \mathbf{U}_{,\mathbf{V}}, \quad \tilde{\mathbf{A}}_i \equiv \mathbf{A}_i \mathbf{A}_0, \quad \tilde{\mathbf{K}}_{ij} \equiv \mathbf{K}_{ij} \mathbf{A}_0,$$

- Equations in entropy variables are a **symmetric parabolic** system:

- ▶ The matrices \mathbf{A}_0 and $\tilde{\mathbf{A}}_i$ are symmetric.
- ▶ The matrix $\tilde{\mathbf{K}} \equiv \begin{pmatrix} \tilde{\mathbf{K}}_{11} & \tilde{\mathbf{K}}_{12} & \tilde{\mathbf{K}}_{13} \\ \tilde{\mathbf{K}}_{21} & \tilde{\mathbf{K}}_{22} & \tilde{\mathbf{K}}_{23} \\ \tilde{\mathbf{K}}_{31} & \tilde{\mathbf{K}}_{32} & \tilde{\mathbf{K}}_{33} \end{pmatrix}$ is symmetric positive semi-definite.

Symmetrized Compressible Navier-Stokes Equations

- Compressible Navier-Stokes equations in the entropy variables:

$$\mathbf{V}^T(\mathbf{x}, t) \equiv \left(-U_5 + \rho_1(\gamma + 1 - s), \quad U_2, \quad U_3, \quad U_4, \quad -U_1 \right) \in \mathbb{R}^5$$

$$s = \ln \left[\frac{(\gamma - 1)\rho_1}{U_1^\gamma} \right], \quad \rho_1 = U_5 - \frac{1}{2U_1}(U_2^2 + U_3^2 + U_4^2)$$

$$\Rightarrow \mathbf{A}_0 \mathbf{V}_{,t} + \tilde{\mathbf{A}}_i \mathbf{V}_{,i} - (\tilde{\mathbf{K}}_{ij} \mathbf{V}_{,j})_{,i} = \mathbf{0}$$

where

$$\mathbf{A}_0 \equiv \mathbf{U}_{,\mathbf{V}}, \quad \tilde{\mathbf{A}}_i \equiv \mathbf{A}_i \mathbf{A}_0, \quad \tilde{\mathbf{K}}_{ij} \equiv \mathbf{K}_{ij} \mathbf{A}_0,$$

- Equations in entropy variables are a **symmetric parabolic** system:

- ▶ The matrices \mathbf{A}_0 and $\tilde{\mathbf{A}}_i$ are symmetric.
- ▶ The matrix $\tilde{\mathbf{K}} \equiv \begin{pmatrix} \tilde{\mathbf{K}}_{11} & \tilde{\mathbf{K}}_{12} & \tilde{\mathbf{K}}_{13} \\ \tilde{\mathbf{K}}_{21} & \tilde{\mathbf{K}}_{22} & \tilde{\mathbf{K}}_{23} \\ \tilde{\mathbf{K}}_{31} & \tilde{\mathbf{K}}_{32} & \tilde{\mathbf{K}}_{33} \end{pmatrix}$ is symmetric positive semi-definite.

Numerical schemes for the compressible Navier-Stokes in the physical entropy variables were studied extensively by Hughes *et al.* [9]



A Stable Galerkin ROM

- Stability analysis dictates that we compute the POD modes and perform the Galerkin projection in the entropy variables.



A Stable Galerkin ROM

- Stability analysis dictates that we compute the POD modes and perform the Galerkin projection in the entropy variables.
- Entropy estimate (Clausius-Duhem inequality): $\frac{d}{dt} \int_{\Omega} \rho_N \eta_N d\Omega \geq 0$



A Stable Galerkin ROM

- Stability analysis dictates that we compute the POD modes and perform the Galerkin projection in the entropy variables.
- Entropy estimate (Clausius-Duhem inequality): $\frac{d}{dt} \int_{\Omega} \rho_N \eta_N d\Omega \geq 0$

Practical Implication:

Building ROM in entropy variables ensures *a priori* that stability property possessed by solutions of the Navier-Stokes equations is automatically inherited by discrete ROM solutions for **any** basis!



A Stable Galerkin ROM

- Stability analysis dictates that we compute the POD modes and perform the Galerkin projection in the entropy variables.
- Entropy estimate (Clausius-Duhem inequality): $\frac{d}{dt} \int_{\Omega} \rho_N \eta_N d\Omega \geq 0$

Practical Implication:

Building ROM in entropy variables ensures *a priori* that stability property possessed by solutions of the Navier-Stokes equations is automatically inherited by discrete ROM solutions for **any** basis!

- Galerkin projection performed in the entropy variables:

$$(\phi_m, \mathbf{A}_0 \mathbf{V}_{M,t}) - \left(\phi_m, \tilde{\mathbf{A}}_i \mathbf{V}_{M,i} \right) + (\phi_{m,i}, \tilde{\mathbf{K}}_{ij} \mathbf{V}_{M,j}) = 0.$$

A Stable Galerkin ROM

- Stability analysis dictates that we compute the POD modes and perform the Galerkin projection in the entropy variables.
- Entropy estimate (Clausius-Duhem inequality): $\frac{d}{dt} \int_{\Omega} \rho_N \eta_N d\Omega \geq 0$

Practical Implication:

Building ROM in entropy variables ensures *a priori* that stability property possessed by solutions of the Navier-Stokes equations is automatically inherited by discrete ROM solutions for **any** basis!

- Galerkin projection performed in the entropy variables:

$$(\phi_m, \mathbf{A}_0 \mathbf{V}_{M,t}) - \left(\phi_m, \tilde{\mathbf{A}}_i \mathbf{V}_{M,i} \right) + (\phi_{m,i}, \tilde{\mathbf{K}}_{ij} \mathbf{V}_{M,j}) = 0.$$

- Substitute modal decomposition $\mathbf{V}_M = \sum_{k=1}^M a_k(t) \phi_k(\mathbf{x})$ to obtain an $M \times M$ **non-linear** dynamical system of the form

$$\sum_{n=1}^M (\phi_m, [\mathbf{A}_0]_M \phi_n) \dot{a}_n = - \left(\phi_m, [\tilde{\mathbf{A}}_i]_M \mathbf{V}_{M,i} \right) - (\phi_{m,i}, [\tilde{\mathbf{K}}_{ij}]_M \mathbf{V}_{M,j})$$



Efficiency: Interpolation of Non-Linear Terms

- Discrete **non-linear** ROM system is of the form:

$$\sum_{n=1}^M (\phi_m, [\mathbf{f}_0(\mathbf{V}_M)]_n) \dot{a}_n = - (\phi_m, \mathbf{f}_1(\mathbf{V}_M)) - \sum_{i=1}^3 (\phi_m, \mathbf{f}_{i+1}(\mathbf{V}_M))$$

where

$$\mathbf{f}_i(\mathbf{V}_M) \equiv \mathbf{f}_i \left(\sum_{m=1}^M a_m(t) \phi_m(\mathbf{x}) \right), \quad i = 0, \dots, 4.$$



Efficiency: Interpolation of Non-Linear Terms

- Discrete **non-linear** ROM system is of the form:

$$\sum_{n=1}^M (\phi_m, [\mathbf{f}_0(\mathbf{V}_M)]_n) \dot{a}_n = - (\phi_m, \mathbf{f}_1(\mathbf{V}_M)) - \sum_{i=1}^3 (\phi_m, \mathbf{f}_{i+1}(\mathbf{V}_M))$$

where

$$\mathbf{f}_i(\mathbf{V}_M) \equiv \mathbf{f}_i \left(\sum_{m=1}^M a_m(t) \phi_m(\mathbf{x}) \right), \quad i = 0, \dots, 4.$$

- Inner products cannot be pre-computed prior to time-integration of ROM system.



Efficiency: Interpolation of Non-Linear Terms

- Discrete **non-linear** ROM system is of the form:

$$\sum_{n=1}^M (\phi_m, [\mathbf{f}_0(\mathbf{V}_M)]_n) \dot{a}_n = - (\phi_m, \mathbf{f}_1(\mathbf{V}_M)) - \sum_{i=1}^3 (\phi_{m,i}, \mathbf{f}_{i+1}(\mathbf{V}_M))$$

where

$$\mathbf{f}_i(\mathbf{V}_M) \equiv \mathbf{f}_i \left(\sum_{m=1}^M a_m(t) \phi_m(\mathbf{x}) \right), \quad i = 0, \dots, 4.$$

- Inner products cannot be pre-computed prior to time-integration of ROM system.
- To recover efficiency, interpolate* non-linear terms:

$$\mathbf{f}_i(\mathbf{V}_M) \approx \sum_{m=1}^M \mathbf{f}_i \left(\sum_{n=1}^M a_n(t) \phi_n(\mathbf{x}_m^{\mathbf{f}_i}) \right) \psi_m^{\mathbf{f}_i}, \quad i = 0, \dots, 4$$

$\mathbf{x}_m^{\mathbf{f}_i}$ = interpolation points for \mathbf{f}_i , $\psi_m^{\mathbf{f}_i}$ = “cardinal functions” computed for \mathbf{f}_i

* Computed via the “best points” interpolation procedure of Peraire, Nguyen *et al.* [5].



Efficiency: Interpolation of Non-Linear Terms

- Discrete **non-linear** ROM system is of the form:

$$\sum_{n=1}^M (\phi_m, [\mathbf{f}_0(\mathbf{V}_M)]_n) \dot{a}_n = - (\phi_m, \mathbf{f}_1(\mathbf{V}_M)) - \sum_{i=1}^3 (\phi_{m,i}, \mathbf{f}_{i+1}(\mathbf{V}_M))$$

where

$$\mathbf{f}_i(\mathbf{V}_M) \equiv \mathbf{f}_i \left(\sum_{m=1}^M a_m(t) \phi_m(\mathbf{x}) \right), \quad i = 0, \dots, 4.$$

- Inner products cannot be pre-computed prior to time-integration of ROM system.
- To recover efficiency, interpolate* non-linear terms:

$$\mathbf{f}_i(\mathbf{V}_M) \approx \sum_{m=1}^M \mathbf{f}_i \left(\sum_{n=1}^M a_n(t) \phi_n(\mathbf{x}_m^{\mathbf{f}_i}) \right) \psi_m^{\mathbf{f}_i}, \quad i = 0, \dots, 4$$

$\mathbf{x}_m^{\mathbf{f}_i}$ = interpolation points for \mathbf{f}_i , $\psi_m^{\mathbf{f}_i}$ = “cardinal functions” computed for \mathbf{f}_i

- ROM ODE system with interpolation:

$$\mathbf{M} \dot{\mathbf{a}}_M + \sum_{i=1}^4 \mathbf{G}^{\mathbf{f}_i} \mathbf{f}_i(\mathbf{D}^{\mathbf{f}_i} \mathbf{a}_M) = \mathbf{0}$$

where \mathbf{M} , $\mathbf{G}^{\mathbf{f}_i}$, $\mathbf{D}^{\mathbf{f}_i}$ are pre-computed in the offline stage of ROM.

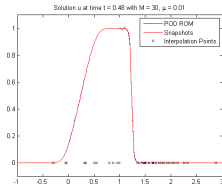
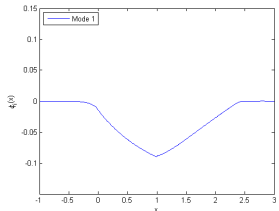


* Computed via the “best points” interpolation procedure of Peraire, Nguyen *et al.* [5].

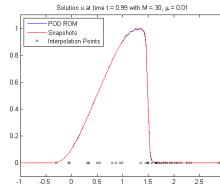
Preliminary Numerical Study 1: Viscous Burgers Equation

$$u_t + \left(\frac{u^2}{2}\right)_x = \mu u_{xx}, \quad -1 < x < 3, \quad 0 < t < T, \\ u(-1, t) = u(3, t) = 0, \quad 0 < t < T,$$

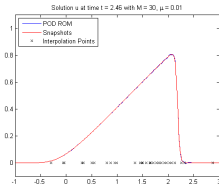
- Initial data: $u(x, 0) = \begin{cases} 0, & x < 0, \\ 1, & 0 \leq x < 1, \\ 0, & x \geq 1, \end{cases}$
- Formation of rarefaction and shock in the $\mu \rightarrow 0$ limit.
- Results shown for $\mu = 0.01$, $M = 30$ modes, computed from $K = 101$ snapshots of ENO-LLF “high fidelity” finite volume solution.



$t = 0.48$



$t = 0.99$

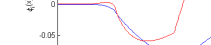


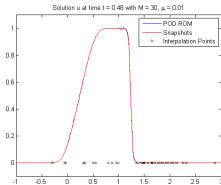
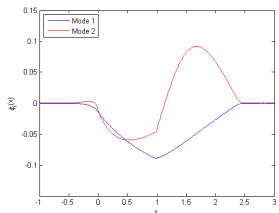
$t = 2.46$

Preliminary Numerical Study 1: Viscous Burgers Equation

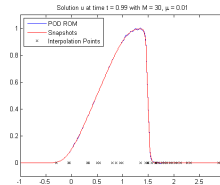
$$u_t + \left(\frac{u^2}{2}\right)_x = \mu u_{xx}, \quad -1 < x < 3, \quad 0 < t < T, \\ u(-1, t) = u(3, t) = 0, \quad 0 < t < T,$$

- Initial data: $u(x, 0) = \begin{cases} 0, & x < 0, \\ 1, & 0 \leq x < 1, \\ 0, & x \geq 1, \end{cases}$
- Formation of rarefaction and shock in the $\mu \rightarrow 0$ limit.
- Results shown for $\mu = 0.01$, $M = 30$ modes, computed from $K = 101$ snapshots of ENO-LLF “high fidelity” finite volume solution.

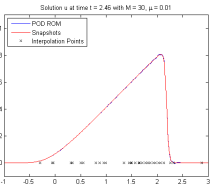




$t = 0.48$



t = 0.99

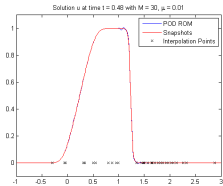


$t = 2.46$

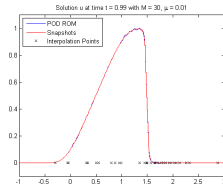
Preliminary Numerical Study 1: Viscous Burgers Equation

$$u_t + \left(\frac{u^2}{2}\right)_x = \mu u_{xx}, \quad -1 < x < 3, \quad 0 < t < T, \\ u(-1, t) = u(3, t) = 0, \quad 0 < t < T,$$

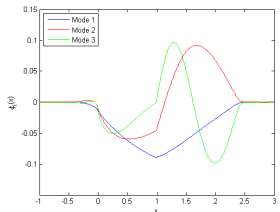
- Initial data: $u(x, 0) = \begin{cases} 0, & x < 0, \\ 1, & 0 \leq x < 1, \\ 0, & x \geq 1, \end{cases}$
- Formation of rarefaction and shock in the $\mu \rightarrow 0$ limit.
- Results shown for $\mu = 0.01$, $M = 30$ modes, computed from $K = 101$ snapshots of ENO-LLF “high fidelity” finite volume solution.



$t = 0.48$



$t = 0.99$

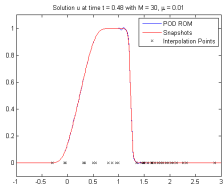


$t = 2.46$

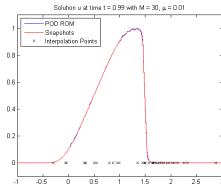
Preliminary Numerical Study 1: Viscous Burgers Equation

$$u_t + \left(\frac{u^2}{2}\right)_x = \mu u_{xx}, \quad -1 < x < 3, \quad 0 < t < T, \\ u(-1, t) = u(3, t) = 0, \quad 0 < t < T,$$

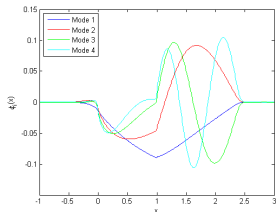
- Initial data: $u(x, 0) = \begin{cases} 0, & x < 0, \\ 1, & 0 \leq x < 1, \\ 0, & x \geq 1, \end{cases}$
- Formation of rarefaction and shock in the $\mu \rightarrow 0$ limit.
- Results shown for $\mu = 0.01$, $M = 30$ modes, computed from $K = 101$ snapshots of ENO-LLF “high fidelity” finite volume solution.



$t = 0.48$



$t = 0.99$

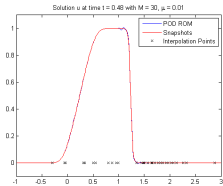
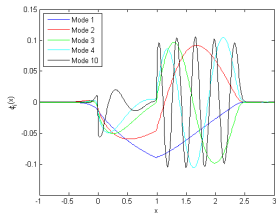


$t = 2.46$

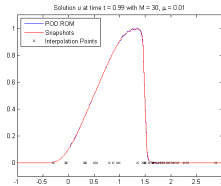
Preliminary Numerical Study 1: Viscous Burgers Equation

$$u_t + \left(\frac{u^2}{2}\right)_x = \mu u_{xx}, \quad -1 < x < 3, \quad 0 < t < T, \\ u(-1, t) = u(3, t) = 0, \quad 0 < t < T,$$

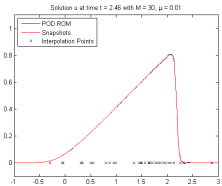
- Initial data: $u(x, 0) = \begin{cases} 0, & x < 0, \\ 1, & 0 \leq x < 1, \\ 0, & x \geq 1, \end{cases}$
- Formation of rarefaction and shock in the $\mu \rightarrow 0$ limit.
- Results shown for $\mu = 0.01$, $M = 30$ modes, computed from $K = 101$ snapshots of ENO-LLF “high fidelity” finite volume solution.



$t = 0.48$



$t = 0.99$



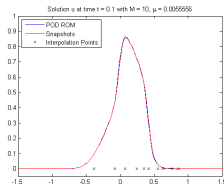
$t = 2.46$

Preliminary Numerical Study 2: Buckley-Leverett Equation

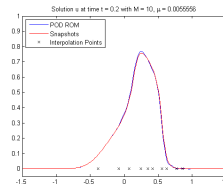
$$u_t + \left(\frac{u^2}{u^2 + (1-u)^2} \right)_x = \mu u_{xx}, \quad -1.5 < x < 1.5, \\ u(-1.5, t) = u(1.5, t) = 0,$$

- Used to model two-phase flow in porous media.
- Highly non-linear, non-convex flux.
- Gaussian initial condition: $u(x, 0) = e^{-16x^2}$.
- Results shown for $\mu = 0.05$, $M = 10$ modes, computed from $K = 50$ snapshots of ENO-LLF “high fidelity” finite volume solution.

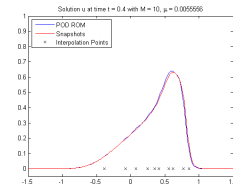
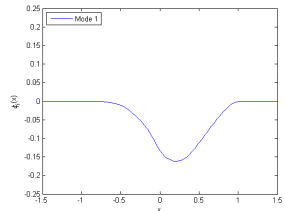




$t_c = 0.1$



$t = 0.2$

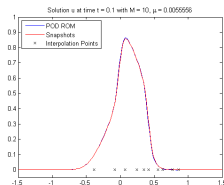
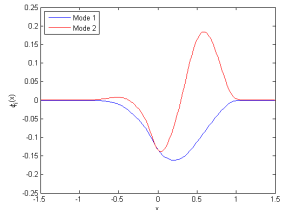


A set of small, semi-transparent navigation icons typically found in Beamer presentations, including icons for back, forward, and search.

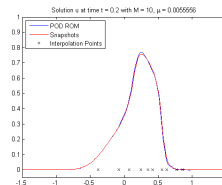
Preliminary Numerical Study 2: Buckley-Leverett Equation

$$u_t + \left(\frac{u^2}{u^2 + (1-u)^2} \right)_x = \mu u_{xx}, \quad -1.5 < x < 1.5, \\ u(-1.5, t) = u(1.5, t) = 0,$$

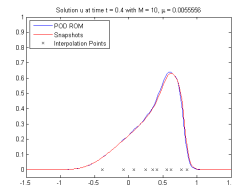
- Used to model two-phase flow in porous media.
- Highly non-linear, non-convex flux.
- Gaussian initial condition: $u(x, 0) = e^{-16x^2}$.
- Results shown for $\mu = 0.05$, $M = 10$ modes, computed from $K = 50$ snapshots of ENO-LLF “high fidelity” finite volume solution.



$t = 0.1$



$t = 0.2$

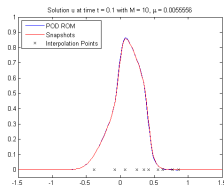
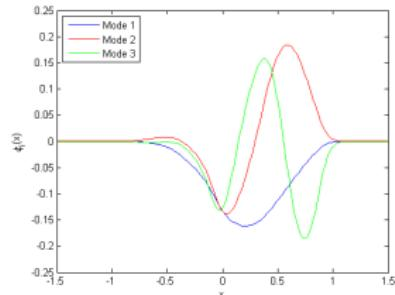


$t = 0.4$

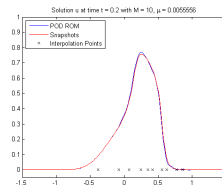
Preliminary Numerical Study 2: Buckley-Leverett Equation

$$u_t + \left(\frac{u^2}{u^2 + (1-u)^2} \right)_x = \mu u_{xx}, \quad -1.5 < x < 1.5, \\ u(-1.5, t) = u(1.5, t) = 0,$$

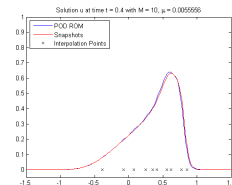
- Used to model two-phase flow in porous media.
- Highly non-linear, non-convex flux.
- Gaussian initial condition: $u(x, 0) = e^{-16x^2}$.
- Results shown for $\mu = 0.05$, $M = 10$ modes, computed from $K = 50$ snapshots of ENO-LLF “high fidelity” finite volume solution.



$t = 0.1$



$t = 0.2$

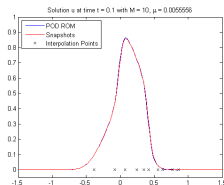
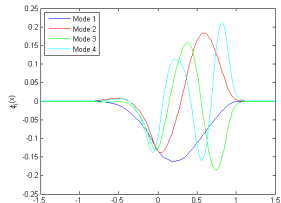


$t = 0.4$

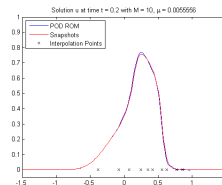
Preliminary Numerical Study 2: Buckley-Leverett Equation

$$u_t + \left(\frac{u^2}{u^2 + (1-u)^2} \right)_x = \mu u_{xx}, \quad -1.5 < x < 1.5, \\ u(-1.5, t) = u(1.5, t) = 0,$$

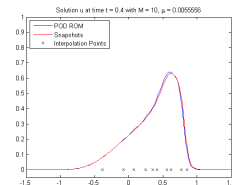
- Used to model two-phase flow in porous media.
- Highly non-linear, non-convex flux.
- Gaussian initial condition: $u(x, 0) = e^{-16x^2}$.
- Results shown for $\mu = 0.05$, $M = 10$ modes, computed from $K = 50$ snapshots of ENO-LLF “high fidelity” finite volume solution.



$t = 0.1$



$t = 0.2$

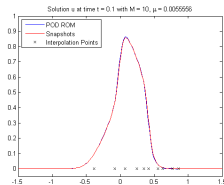


Preliminary Numerical Study 2: Buckley-Leverett Equation

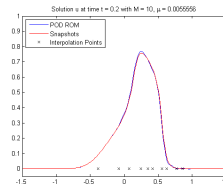
$$u_t + \left(\frac{u^2}{u^2 + (1-u)^2} \right)_x = \mu u_{xx}, \quad -1.5 < x < 1.5, \\ u(-1.5, t) = u(1.5, t) = 0,$$

- Used to model two-phase flow in porous media.
- Highly non-linear, non-convex flux.
- Gaussian initial condition: $u(x, 0) = e^{-16x^2}$.
- Results shown for $\mu = 0.05$, $M = 10$ modes, computed from $K = 50$ snapshots of ENO-LLF “high fidelity” finite volume solution.

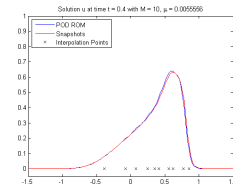
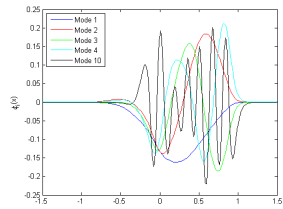




$t_c = 0.1$



$t = 0.2$



A set of small, semi-transparent navigation icons typically found in Beamer presentations, including icons for back, forward, and search.

Summary & Future Work

This Paper: Extension stable Galerkin ROM based on the continuous projection method previously developed [2-4] for **linearized** compressible flow equations to ***non-linear*** equations.

- Implement the entropy stable compressible Navier-Stokes ROM formulated in this paper; compare to other non-linear model reduction techniques (e.g., discrete Galerkin projection approach).
- Extend model reduction technique to allow incorporation of stabilization and shock-capturing operators [9].
- Extend model reduction technique to allow incorporation of turbulence models (LES, RANS-LES).
- Explore robustness of ROM with respect to parameter changes (reduced basis interpolation techniques [7]).
- Investigate the viability of the POD basis for non-linear problems: are there “better” bases to employ (e.g., balanced POD)? (entropy stability result is **basis independent!**)

References

(www.stanford.edu/~irinak)

- [1] I. Kalashnikova, M.F. Barone. "Efficient Non-Linear POD Reduced Order Models with Stable Penalty Enforcement of Boundary Conditions". Submitted to *Int. J. Numer. Meth. Engng.* (under review).
- [2] I. Kalashnikova, M.F. Barone. "On the Stability and Convergence of a Galerkin Reduced Order Model (ROM) of Compressible Flow with Solid Wall and Far-Field Boundary Treatment". *Int. J. Numer. Meth. Engng.* **83** (2010) 1345-1375.
- [3] M.F. Barone, I. Kalashnikova, D.J. Segalman, H. Thornquist. "Stable Galerkin Reduced Order Models for Linearized Compressible Flow". *J. Comput. Phys.* **288** (2009) 1932-1946.
- [4] M.F. Barone, D.J. Segalman, H. Thornquist, I. Kalashnikova. "Galerkin Reduced Order Models for Compressible Flow with Structural Interaction". *AIAA Paper No. 2008-0612*, 46th AIAA Aerospace Science Meeting and Exhibit, Reno, NV (Jan. 2008).
- [5] N.C. Nguyen, J. Peraire. "An efficient reduced-order modeling approach for non-linear parametrized partial differential equations". *Int. J. Numer. Meth. Engng.* **76**:27–55 (2008).
- [6] A. Harten. "On the symmetric form of systems of conservation laws with entropy". *J. Comput. Phys.* **49**: 151–164 (1983).
- [7] D. Amsallem, C. Farhat. "An Interpolation Method for Adapting Reduced-Order Models and Application to Aeroelasticity". *AIAA Journal*, **46** (2008) 1803–1813.
- [8] S.W. Bova, G.F. Carey. "An entropy variable formulation and applications for the two-dimensional shallow water equations". *Int. J. Numer. Meth. Fluids* **23** 29–46 (1996).
- [9] F. Shakib, T.J.R. Hughes, Z. Johan. "A new finite element formulation for computational fluid dynamics: X. The compressible Euler and Navier-Stokes equations". *Comput. Meth. Appl. Mech. Engng.* **89** 141–219 (1991).

References

(www.stanford.edu/~irinak)

- [1] I. Kalashnikova, M.F. Barone. "Efficient Non-Linear POD Reduced Order Models with Stable Penalty Enforcement of Boundary Conditions". Submitted to *Int. J. Numer. Meth. Engng.* (under review).
- [2] I. Kalashnikova, M.F. Barone. "On the Stability and Convergence of a Galerkin Reduced Order Model (ROM) of Compressible Flow with Solid Wall and Far-Field Boundary Treatment". *Int. J. Numer. Meth. Engng.* **83** (2010) 1345-1375.
- [3] M.F. Barone, I. Kalashnikova, D.J. Segalman, H. Thornquist. "Stable Galerkin Reduced Order Models for Linearized Compressible Flow". *J. Comput. Phys.* **288** (2009) 1932-1946.
- [4] M.F. Barone, D.J. Segalman, H. Thornquist, I. Kalashnikova. "Galerkin Reduced Order Models for Compressible Flow with Structural Interaction". *AIAA Paper No. 2008-0612*, 46th AIAA Aerospace Science Meeting and Exhibit, Reno, NV (Jan. 2008).
- [5] N.C. Nguyen, J. Peraire. "An efficient reduced-order modeling approach for non-linear parametrized partial differential equations". *Int. J. Numer. Meth. Engng.* **76**:27–55 (2008).
- [6] A. Harten. "On the symmetric form of systems of conservation laws with entropy". *J. Comput. Phys.* **49**: 151–164 (1983).
- [7] D. Amsallem, C. Farhat. "An Interpolation Method for Adapting Reduced-Order Models and Application to Aeroelasticity". *AIAA Journal*, **46** (2008) 1803–1813.
- [8] S.W. Bova, G.F. Carey. "An entropy variable formulation and applications for the two-dimensional shallow water equations". *Int. J. Numer. Meth. Fluids* **23** 29–46 (1996).
- [9] F. Shakib, T.J.R. Hughes, Z. Johan. "A new finite element formulation for computational fluid dynamics: X. The compressible Euler and Navier-Stokes equations". *Comput. Meth. Appl. Mech. Engng.* **89** 141–219 (1991).

Thank you! Questions?

ikalash@sandia.gov



Symmetrizing Matrix \mathbf{A}_0

- Introduce the notation:

$$\begin{aligned}\bar{\gamma} &= \gamma - 1, & k_1 &= \frac{1}{2V_5}(V_2^2 + V_3^2 + V_4^2), & k_2 &= k_1 - \gamma, \\ k_3 &= k_1^2 - 2\gamma k_1 + \gamma, & k_4 &= k_2 - \bar{\gamma}, & k_5 &= k_2^2 - \bar{\gamma}(k_1 + k_2), \\ c_1 &= \bar{\gamma}V_5 - V_2^2, & d_1 &= -V_2V_3, & e_1 &= V_2V_5, \\ c_2 &= \bar{\gamma}V_5 - V_3^2, & d_2 &= -V_2V_4, & e_2 &= V_3V_5, \\ c_3 &= \bar{\gamma}V_5 - V_4^2, & d_3 &= -V_3V_4, & e_3 &= V_4V_5.\end{aligned}$$

$$\rho_1 = \left[\frac{\gamma - 1}{(-V_5)^\gamma} \right]^{1/(\gamma-1)} \exp\left(\frac{-s}{\gamma - 1}\right).$$

- Inverse transformation $\mathbf{V} \rightarrow \mathbf{U}$:

$$\mathbf{U}^T = \rho_1 \left(\begin{array}{ccccc} -V_5, & V_2, & V_3, & V_4, & 1 - \frac{1}{2V_5}(V_2^2 + V_3^2 + V_4^2) \end{array} \right)$$

- Symmetrizing matrix \mathbf{A}_0 :

$$\mathbf{A}_0 = \mathbf{U}_{,\mathbf{V}} = \frac{\rho_1}{\bar{\gamma}V_5} \begin{pmatrix} -V_5^2 & e_1 & e_2 & e_3 & V_5(1 - k_1) \\ c_1 & d_1 & d_2 & & V_2k_2 \\ & c_2 & d_3 & & V_3k_2 \\ & c_3 & & V_4k_2 & \\ & & & -k_3 & \end{pmatrix}$$

symm.



Jacobians of Symmetrized Euler Fluxes $\tilde{\mathbf{A}}_i$

$$\tilde{\mathbf{A}}_1 = \tilde{\mathbf{F}}_{1,\mathbf{v}} = \frac{\rho_1}{\bar{\gamma}V_5^2} \begin{pmatrix} e_1 V_5 & c_1 V_5 & d_1 V_5 & d_2 V_5 & k_2 e_1 \\ & -(c_1 + 2\bar{\gamma}V_5)V_2 & -c_1 V_3 & -c_1 V_4 & c_1 k_2 + \bar{\gamma}V_2^2 \\ & & -c_2 V_2 & -d_1 V_4 & k_4 d_1 \\ \text{symm.} & & & -c_3 V_2 & k_4 d_2 \\ & & & & k_5 V_2 \end{pmatrix},$$

$$\tilde{\mathbf{A}}_2 = \tilde{\mathbf{F}}_{2,\mathbf{v}} = \frac{\rho_1}{\bar{\gamma}V_5^2} \begin{pmatrix} e_2 V_5 & d_1 V_5 & c_2 V_5 & d_3 V_5 & k_2 e_2 \\ & -c_1 V_3 & -c_2 V_2 & -d_1 V_4 & k_4 d_1 \\ & & -(c_2 + 2\bar{\gamma}V_5)V_3 & -c_2 V_4 & c_2 k_2 + \bar{\gamma}V_3^2 \\ \text{symm.} & & & -c_3 V_3 & k_4 d_3 \\ & & & & k_5 V_3 \end{pmatrix},$$

$$\tilde{\mathbf{A}}_3 = \tilde{\mathbf{F}}_{3,\mathbf{v}} = \frac{\rho_1}{\bar{\gamma}V_5^2} \begin{pmatrix} e_3 V_5 & d_2 V_5 & 7d_3 V_5 & c_3 V_5 & k_2 e_3 \\ & -c_1 V_4 & & -d_2 V_3 & -c_3 V_2 \\ & & & -c_2 V_4 & -c_3 V_3 \\ & & & & k_4 d_2 \\ \text{symm.} & & & & k_4 d_3 \\ & & & & -(c_3 + 2\bar{\gamma}V_5)V_4 \\ & & & & c_3 k_2 + \bar{\gamma}V_4^2 \\ & & & & k_5 V_4 \end{pmatrix}.$$

Symmetrized Viscous and Heat Fluxes $\tilde{\mathbf{K}}_{ij}$

$$\tilde{\mathbf{K}}_{11} = \frac{1}{V_5^3} \begin{pmatrix} 0 & 0 & 0 & 0 & 0 \\ 0 & -(\gamma - 2\mu)V_5^2 & 0 & 0 & (\lambda + 2\mu)e_1 \\ 0 & 0 & -\mu V_5^2 & 0 & \mu e_2 \\ 0 & 0 & 0 & -\mu V_5^2 & \mu e_3 \\ 0 & (\lambda + 2\mu)e_1 & \mu e_2 & \mu e_3 & -\left[(\lambda + 2\mu)V_2^2 + \mu(V_3^2 + V_4^2) - \frac{\gamma\mu V_5}{Pr}\right] \end{pmatrix},$$

$$\tilde{\mathbf{K}}_{12} = \frac{1}{V_5^3} \begin{pmatrix} 0 & 0 & 0 & 0 & 0 \\ 0 & 0 & -\lambda V_5^2 & 0 & \lambda e_2 \\ 0 & -\mu V_5^2 & 0 & 0 & \mu e_1 \\ 0 & 0 & 0 & 0 & 0 \\ 0 & \mu e_2 & \lambda e_1 & 0 & (\lambda + \mu)d_1 \end{pmatrix},$$

$$\tilde{\mathbf{K}}_{13} = \frac{1}{V_5^3} \begin{pmatrix} 0 & 0 & 0 & 0 & 0 \\ 0 & 0 & 0 & -\lambda V_5^2 & \lambda e_3 \\ 0 & 0 & 0 & 0 & 0 \\ 0 & -\mu V_5^2 & 0 & 0 & \mu e_1 \\ 0 & \mu e_3 & 0 & \lambda e_1 & (\lambda + \mu)d_2 \end{pmatrix},$$

Symmetrized Viscous and Heat Fluxes $\tilde{\mathbf{K}}_{ij}$ (Continued)

$$\tilde{\mathbf{K}}_{22} = \frac{1}{V_5^3} \begin{pmatrix} 0 & 0 & 0 & 0 & 0 \\ 0 & -\mu V_5^2 & 0 & 0 & \mu e_1 \\ 0 & 0 & -(\lambda + 2\mu) V_5^2 & 0 & (\lambda + 2\mu) e_2 \\ 0 & 0 & 0 & -\mu V_5^2 & \mu e_3 \\ 0 & \mu e_1 & (\lambda + 2\mu) e_2 & \mu e_3 & - \left[(\lambda + 2\mu) V_3^2 + \mu (V_2^2 + V_4^2) - \frac{\gamma \mu V_5}{Pr} \right] \end{pmatrix},$$

$$\tilde{\mathbf{K}}_{23} = \frac{1}{V_5^3} \begin{pmatrix} 0 & 0 & 0 & 0 & 0 \\ 0 & 0 & 0 & 0 & 0 \\ 0 & 0 & 0 & -\lambda V_5^2 & \lambda e_3 \\ 0 & 0 & -\mu V_5^2 & 0 & \mu e_2 \\ 0 & 0 & \mu e_3 & \lambda e_2 & (\lambda + \mu) d_3 \end{pmatrix},$$

$$\tilde{\mathbf{K}}_{33} = \frac{1}{V_5^3} \begin{pmatrix} 0 & 0 & 0 & 0 & 0 \\ 0 & -\mu V_5^2 & 0 & 0 & \mu e_1 \\ 0 & 0 & -\mu V_5^2 & 0 & \mu e_2 \\ 0 & 0 & 0 - (\lambda + 2\mu) V_5^2 & (\lambda + 2\mu) e_3 & - \left[(\lambda + 2\mu) V_4^2 + \mu (V_2^2 + V_3^2) - \frac{\gamma \mu V_5}{Pr} \right] \\ 0 & \mu e_1 & \mu e_2 & (\lambda + 2\mu) e_3 & \end{pmatrix},$$

$$\tilde{\mathbf{K}}_{21} = \tilde{\mathbf{K}}_{12}^T, \quad \tilde{\mathbf{K}}_{31} = \tilde{\mathbf{K}}_{13}^T, \quad \tilde{\mathbf{K}}_{32} = \tilde{\mathbf{K}}_{23}^T.$$

Semi-Discrete ROM System Matrices

- Semi-discrete ROM ODE system following interpolation:

$$\mathbf{M}\dot{\mathbf{a}}_M + \sum_{i=1}^4 \mathbf{G}^{\mathbf{f}_i} \mathbf{f}_i(\mathbf{D}^{\mathbf{f}_i} \mathbf{a}_M) = \mathbf{0},$$

- $\mathbf{G}^{\mathbf{f}_i}$ matrices:

$$\mathbf{G}_{l,[5(m-1)+1:5m]}^{\mathbf{f}_1} = \int_{\Omega} (\phi_l^1 \psi_m^{f_1^1}, \phi_l^2 \psi_m^{f_1^2}, \phi_l^3 \psi_m^{f_1^3}, \phi_l^4 \psi_m^{f_1^4}, \phi_l^5 \psi_m^{f_1^5}) d\Omega,$$

$$\mathbf{G}_{l,[5(m-1)+1:5m]}^{\mathbf{f}_{i+1}} = \int_{\Omega} (\phi_{l,i}^1 \psi_m^{f_{i+1}^1}, \phi_{l,i}^2 \psi_m^{f_{i+1}^2}, \phi_{l,i}^3 \psi_m^{f_{i+1}^3}, \phi_{l,i}^4 \psi_m^{f_{i+1}^4}, \phi_{l,i}^5 \psi_m^{f_{i+1}^5}) d\Omega, i = 1, 2, 3$$

for $l, m = 1, \dots, M$.

- Mass matrix \mathbf{M} : for $k = 1, \dots, M$,

$$\mathbf{M}_{[1:M],k} = \mathbf{G}^{[\mathbf{f}_0]_k} [\mathbf{f}_0]_k \left(\mathbf{D}^{[\mathbf{f}_0]_k} \mathbf{a}_M \right),$$

- $\mathbf{D}^{\mathbf{f}_i}$ matrices:

$$\mathbf{D}^{\mathbf{f}_i} \equiv \begin{pmatrix} \phi_1 \left(\mathbf{x}_1^{\mathbf{f}_i} \right) & \dots & \phi_M \left(\mathbf{x}_1^{\mathbf{f}_i} \right) \\ \vdots & \ddots & \vdots \\ \phi_1 \left(\mathbf{x}_M^{\mathbf{f}_i} \right) & \dots & \phi_M \left(\mathbf{x}_M^{\mathbf{f}_i} \right) \end{pmatrix}$$